

**International Journal of
Engineering Research and Science & Technology**



ISSN : 2319-5991

www.ijerst.com

Email: editor@ijerst.com or editor.ijerst@gmail.com

ENHANCED DESIGN APPROACHES FOR AN LLC RESONANT CONVERTER IN PEM ELECTROLYZER APPLICATIONS

^{#1}V.M. Ramaapriya, Research scholar, Dept. of EEE, Bharath University, Chennai.

^{#2}Dr. P. Chandrasekhar, professor, Dept. of EEE, Adams Engineering college, Paloncha.

ABSTRACT: A resonant LLC converter is suggested in this study as a way to power a proton exchange membrane (PEM) electrolyzer. voltage overshoots must be avoided, the PEM needs a low voltage with a high current, output voltage disturbance must be kept to a minimum, and the converter's dynamic behavior must be overdamped. The design of the converter cuts down on switching and reverse recovery losses, which lets it meet the requirements of the design. The transmission losses in the output rectifier have the biggest effect on how well it works.

Keywords: PEM electrolyzer; LLC converter, Zero Voltage Switching, energy efficiency.

1. INTRODUCTION

Hydrogen, the universe's most essential element, can store and transfer energy. Unfortunately, hydrogen cannot exist on its own in the natural world. It can only be produced primarily by fusing oxygen in water (H₂O) with carbon, which can be found in hydrocarbons or natural gas.

Only 4% of the hydrogen that may be generated from fossil fuels such as oil and natural gas can be produced using water electrolysis. This is a small amount of hydrogen. The low cost of fossil fuels is the primary driver of this. Electrolyzers are necessary for water electrolysis, which can be costly. However, employing renewable energy sources (RES) to provide power for water electrolysis allows for the production of green hydrogen, which is better for the environment.

There are three types of electrolyzers: solid oxide (SO), proton exchange membrane (PEM), and alkaline. There are peculiarities in how these devices transport ions and electrolytes. Purchases of PEM and alkaline technologies are feasible. To operate, a DC voltage (few volts to hundreds of volts) and DC current (tens of amps to thousands of amps) are required. As a result, having a power adapter is vital.

AC/DC converters are required when the power source is a wind turbine or a power grid. On the

other side, DC/DC converters can be used in tandem with solar panels. When employing power converters, it is critical to consider how voltage and current fluctuations affect the power source and electrolyzer. The negative effects of current ripple from power electronics on electrolyzer energy efficiency and specific energy consumption have been extensively reported in the literature.

Another issue is the efficiency with which energy is converted. The power converter must be as efficient as possible in order to remain competitive. Because a large voltage reduction ratio is required, operating the electrolyzer at a low voltage is challenging. This indicates that limiting excessive currents is required to achieve the rated power.

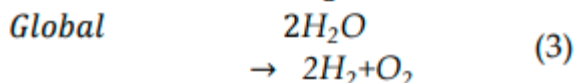
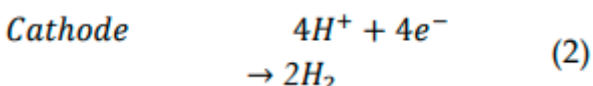
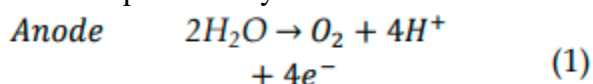
Resonant converters can be utilized in either a series (SRC) or parallel (PRC) architecture to reduce switching losses. The reason for this is that they permitted the power switch to vary depending on the voltage or current null. However, they struggle to retain control at low loads and are only useful at the resonance frequency. Despite their complicated construction, LLC resonant converters are more versatile in use. This is because they use the transformer's magnetizing inductance.

LLCs have numerous applications and can be utilized in both high- and low-power settings. For example, proposes employing a hybrid LLC resonant converter with three separate modes of operation to recharge electric vehicles while they are in motion, while employs a three-level system for a variety of input voltage applications. Addresses using an LLC converter as the DC/DC converter's front end. To achieve a high step-down ratio, combine an LLC converter with a partial power conversion. In, an LLC converter-based power source for LED illumination is suggested. However, there is currently no study on employing an LLC conversion to power an electrolyzer. In this situation, additional constraints such as decreased output voltage dispersion and overdamped response must be considered.

This project aims to develop an LLC converter for a proton exchange membrane (PEM) electrolyzer. This converter reduces switching losses by utilizing resonance as well as the zero voltage switching (ZVS) function of power switches. The design takes into account a DC source from the single-phase power grid as well as the load characteristics.

2. PRINCIPAL FEATURES OF AN ELECTROLYZER

To separate the gas that is produced and to insulate the electrodes from one another, proton exchange membrane electrolyzers use solid polymer electrolytes (SPE) to move protons from the anode to the cathode. Let me explain the chemical process to you:



A molecule of water is broken up into oxygen and positively charged protons, which flow into the anode (Eq. 1). Finally, the protons go through the SPE and reach the cathode. There, they combine with electrons from the power source to create hydrogen, as shown in (2). It's important to note that the world reaction (see equation (3)) only makes oxygen, which means there is no pollution. A proton exchange membrane is used in Figure 1 to show how a water electrolyzer works.

The process in (1) needs Gibbs energy (237 kJ.mol⁻¹) and gives off heat (48.6 kJ.mol⁻¹). Lastly, Faraday efficiency is the term for the fact that not all of the electrons that come from the power source are turned into hydrogen.

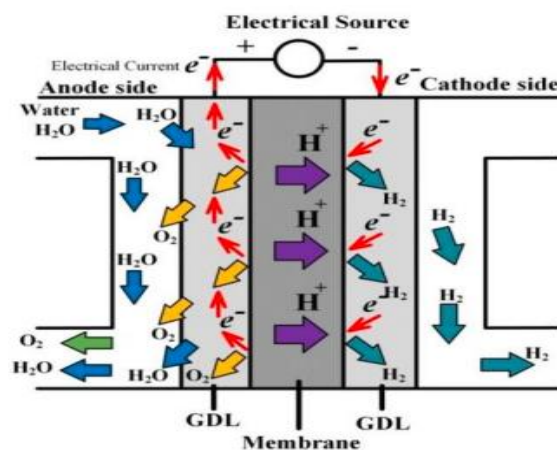


Fig.1. Operation principle for a PEM electrolyzer
The electrolyzer under study

An electrolyzer with the product code 1021882 and manufactured by Fuel Cell Store, the QL-300 PEM Hydrogen Generator, will be supplied by the proposed converter. It generates hydrogen that is exceedingly pure (99.999%) through the utilization of SPE/PEM technology. The QL-300 is capable of producing an output pressure of 310 ml/min and necessitates 150W of power to operate. The grid acquires the standard configuration from a converter supplied by the manufacturer. However, it was transmitted without the necessary documentation for this research endeavor.

Power source. a voltage of at least 5V is necessary at the input terminals for DC power of

approximately 45 amps of current). In graphic form, Figure 2 illustrates the electrolyzer.



Fig.2. External view of the QL-300 electrolyzer

The LLC resonant half-bridge converter

The electrolyzers are powered by the resonant LLC converter in half-bridge arrangement, as illustrated in. The electrical configuration is illustrated in Figure 3. There are three primary components that can be identified: the resonant circuit, the secondary side of the converter, and the half-bridge.

The half-bridge

The half-bridge is intended to generate a voltage that is a single-pole square wave. It is composed of two MOSFETs that are both operational at least half of the time. Cross-conduction can be prevented, and the ZVS condition, which reduces switching losses, can be achieved by allowing a sufficient amount of time between two transitions.

The resonant circuit.

There are two inductors and a resonant capacitor in the resonant circuit. The first inductor is a different part, while the second one is made from the magnetizing inductance of the transformer. The half-bridge and the load are linked by the resonance circuit.

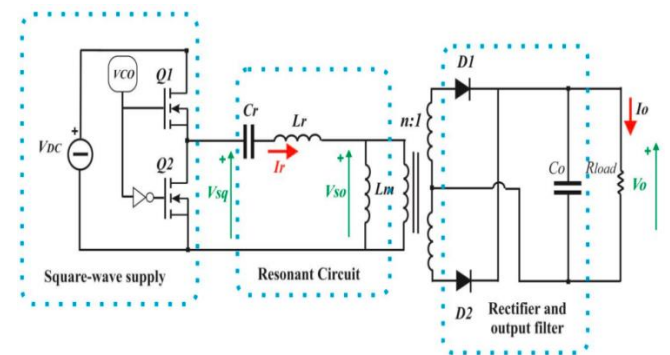
The resonance current makes it easier for energy to get to the transformer and for ZVS to be acquired. The transformer drops the AC voltage and makes sure there is no galvanic separation.

The secondary side

A full-wave rectifier with a center tap design transforms the transformer output voltage to direct current (DC). An output capacitor lowers voltage disturbance as much as possible before the power reaches the electrolyzer.

Operating principle

When a conventional series resonant converter (SRC) is operating at its correct frequency, there is very little resistance. When you go away from the resonant frequency, the selected feature increases the impedance.



The current going to the load is determined by the load's impedance as well as the impedance of the resonant circuit at the square wave source frequency. To accommodate for variations in input and output, a wide variety of input rates is required.

It has two primary frequencies:

f_o , which is the resonant frequency of an SRC and is determined by the inductor and capacitor L_r and C_r , respectively, as shown in (1), and f_p , which is determined by the transformer's magnetizing inductance L_m , as shown in (2).

$$f_o = \frac{1}{2\pi\sqrt{L_r C_r}} \tag{1}$$

$$f_p = \frac{1}{2\pi\sqrt{(L_r + L_m) C_r}} \tag{2}$$

As the load changes, the resonance frequency (f_{co}) changes from f_p to f_o . $f_{co}=f_p$ when there is no load, but $f_{co}=f_o$ when there is a short circuit. In the range $f_p \leq f_{co} \leq f_o$, this feature describes a

group of curves. However, the design process is a lot more complicated.

The design factors that matter are the current going through the output rectifier diodes, the voltage across the MOSFETs when they switch on and off to achieve ZVS, and the currents that make the transformer resonate and magnetize.

When the switching frequency is equal to f_0 , the resonant current and the magnetizing current are equal. This means that no power is sent to the load. Because of this, Q1 is turned off. A delay in the turn-on of Q2 can be used to create the ZVS situation. Soft commutating diodes D1 and D2 can make ZVS even if the switching frequency is less than f_0 . This is possible because they have no current flowing through them. When these diodes work in discontinuous mode, there is more current in the resonant circuit to balance the energy to the load and more conduction losses in the main.

There will be a second track set up. In the end, when the change frequency goes over f_0 , there will be less circulating current in both the main and secondary circuits. This means that there will be less conduction loss. However, because they don't have gentle communication, rectifier diodes will have reverse recovery losses.

The ZVS condition may still be met by MOSFETs.

The LLC converter is designed to work close to f_0 and uses a gain function that depends on the settings of the converter. To find the transfer function, use the first approximation method (FHA). If the converter works close to f_0 , the current in the resonant circuit can be thought of as completely straight. A linear sinusoidal circuit, shown in Figure 4b, can be used instead of the LLC's corresponding circuit, shown in Figure 4a. When the circuit needs power, V_{ge} is the basic part of V_{sq} , and V_{oe} is the basic part of V_{so} .

Using FHA in the following way will help you figure out the converter's transfer function and gain:

$$M_{g_DC} = \frac{V_o \cdot n}{V_{DC}/2} \tag{3}$$

where V_{DC} stands for the input DC voltage and V_o stands for the output DC voltage, and n is the transformer's number of turns. You can change the DC values of V_o and V_{DC} in the circuit shown in Figure 4b to the following RMS values:

$$M_{g_DC} = \frac{V_o \cdot n}{V_{DC}/2} \approx M_{g_sw} = \frac{V_{so}}{V_{sq}} \approx M_{g_AC} = \frac{V_{oe}}{V_{ge}} \tag{4}$$

Finally the gain can be calculated:

$$M_{g_DC} = \frac{V_{oe}}{V_{ge}} = \left| \frac{(j\omega L_m) \parallel R_e}{(j\omega L_m) \parallel R_e + j\omega L_r + \frac{1}{j\omega C_r}} \right| \tag{5}$$

Eq. (4) gives the output voltage by the knowledge of M_g , n , and V_{in} .

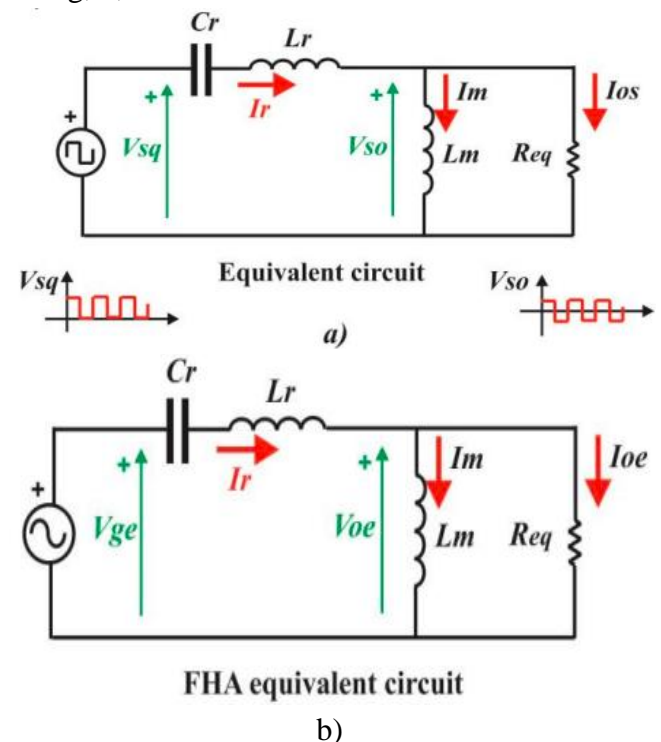


Fig. 4. a) equivalent circuit of the LLC converter, b) FHA circuit model of the LLC converter

To more effectively elucidate equation (5), it is possible to employ normalized numbers in place of real ones. The quality factor (Q_e), the switching frequency to resonant frequency (f_n), and the ratio

of the magnetizing inductance to the resonant inductance (L_n) are the three variables.

$$f_n = \frac{f_{sw}}{f_o} \quad (6)$$

$$L_n = \frac{L_m}{L_r} \quad (7)$$

$$Q_e = \frac{\sqrt{L_r/C_r}}{R_e} \quad (8)$$

In this way, eq. (5) becomes:

$$M_g = \left| \frac{L_n \cdot f_n^2}{[(L_n + 1) \cdot f_n^2 - 1] + j[(f_n^2 - 1) \cdot f_n \cdot Q_e \cdot L_n]} \right| \quad (9)$$

And the output voltage is given by:

$$V_o = M_g \cdot \frac{1}{n} \cdot \frac{V_{DC}}{2} \quad (10)$$

The transfer function M_g can be graphed as a function of frequency, with L_n and Q_e serving as parameters. Design of the LLC resonant converter

3. REVIEW OF LITERATURE

B. Yodwong, D. Guilbert, M. Phattanasak, W. Kaewmanee, M. Hinaje, and G. Vitale reviewed PEM Electrolyzer Modeling for Power Electronics Control in 2020. We study modeling and control methods for PEM electrolyzer integration with power electronics systems in this paper. The abstract likely underlines the necessity of precise modeling in enhancing PEM electrolyzer efficiency and stability for renewable energy hydrogen production.

S. Hiva Kumar and V. Himabindu's 2019 paper analyzes PEM water electrolysis hydrogen generation in detail. PEM electrolyzer basics, technology, and hydrogen generating applications are discussed in this overview. The abstract likely summarizes PEM electrolyzers' essential components and operations, emphasizing its hydrogen generating efficiency, reliability, and sustainability. It highlights material and design

improvements to PEM system performance and longevity.

A. Poullikkas and P. Nikolaidis' 2017 research compares hydrogen generation technologies. Hydrogen generation methods are assessed for efficiency, cost, scalability, and environmental impact. The abstract may encompass steam methane reforming, coal gasification, biomass gasification, electrolysis (alkaline and proton exchange membrane), photoelectrochemical, and biological hydrogen production methods. It compares each method's merits and cons to current technology and market demands.

M. Carmo, D. Fritz, J. Mergel, and D. Stolten's 2013 study examines PEM water electrolysis. PEM electrolyzer basics, technical breakthroughs, and hydrogen generating applications are covered in this overview. The abstract may discuss PEM electrolyzers' efficiency, response time, and renewable energy integration. Recent materials science improvements in catalysts, membranes, and other components improve PEM system performance and longevity.

D. Falcão; A. Pinto. PEM electrolyzer modeling recommendations for beginners. Hydrogen production optimization requires 2020 PEM electrolyzer modeling. The abstract likely includes PEM electrolyzer operation, electrochemical reactions, key components, and system dynamics. It weighs the merits and downsides of simplified theoretical models versus complex computational simulations.

B. Yodwong, D. Guilbert, M. Phattanasak, W. Kaewmanee, M. Hinaje, and G. Vitale's 2020 paper discusses electrolyzer AC-DC converter norms and issues. The abstract likely covers how AC-DC converters boost hydrogen electrolyzer efficiency. It examines how converter topologies, design considerations, and performance measurements affect electrolyzer system reliability and efficiency. The article may explore power density, control, and renewable energy integration converter design advancements.

In 2015, J. Solanki, P. Wallmeier, J. Böcker, A. Averberg, and N. Fröhleke examined cutting-edge high-current variable-voltage rectifiers. As the abstract implies, industrial applications requiring high current and changeable voltage require rectifiers.

J. Solanki, N. Fröhleke, J. Böcker, and P. Wallmeier compared high-power, high-current thyristor-rectifiers to hybrid filters and chopper-rectifiers in 2013. The abstract likely stresses the need of selecting the correct rectification procedure for difficult electrical circumstances.

J. Rodriguez, J. Pontt, C. Silva, E. Wiechmann, P. Hammond, F. Santucci, R. Alvarez, R. Musalem, S. Kouro, and P. Lezana provided a comprehensive study of huge current rectifiers in 2005, focusing on current and future. The abstract may emphasize huge current rectifiers' role in power transmission, renewable energy integration, and electric car charging.

The hybrid filter implementation for a 12-pulse thyristor rectifier delivering high-current variable-voltage DC demand was described by J. Solanki, N. Fröhleke, and J. Böcker in 2015. The abstract may emphasise hybrid filters under challenging electrical settings to increase thyristor rectifier performance and efficiency.

J. Koponen, V. Ruuskanen, A. Kosonen, M. Niemela, and J. Ahola studied converter topology and alkaline water electrolyzer energy consumption in 2019. Electrolyzer energy efficiency is crucial for sustained hydrogen production, hence the abstract may focus converter topologies.

The 2017 paper by Z. Dobó and Á. Palotás explores the impact of current fluctuation on alkaline water electrolysis efficiency. The study may measure current fluctuations' effects on electrolyzer performance using practical and theoretical modeling. Electrolysis efficiency and hydrogen production depend on continuous current supply, according to the abstract.

V. Ruuskanen, J. Koponen, A. Kosonen, M. Niemelä, J. Ahola, and A. Hämäläinen studied water electrolyzers' reactive power and thyristor converter power quality in 2020. The abstract advises studying thyristor-driven electrolyzer power quality and reactive power use. Experimental and theoretical tests can determine how converter operation influences grid reactive power exchange and power quality. Electrolyzer system design and operation are optimized for grid compatibility and performance by this study. Functional circuit locks may be used in LLC power converter design in the 2021 document "Design Reviews – Functional Circuit locks, Designing an LLC Resonant Half-Bridge Power Converter". The abstract may explain how functional circuit locks protect power converters. LLC resonant half-bridge converter design, operation, and performance evaluation may emphasize efficiency, reliability, and functionality. Additionally, the study may examine power converter functional circuit lock design and implementation issues, opportunities, and research goals. This research helps engineers and researchers build superior power electronics systems.

J. H. Jung and J. G. Kwon released LLC resonant converter theoretical analysis and optimal design in September 2007. The abstract may describe LLC resonant converters' power electronics and industrial applications. A research may analyze LLC resonant converter theory, including operating principles, major components, and performance. The research may also improve LLC resonant converter efficiency, power density, and cost. Power electronics researchers and engineers use this work to optimize LLC resonant converter performance.

In 2012, A. Hillers, D. Christen, and J. Biela created an efficient bidirectional isolated LLC resonant converter. The abstract may highlight LLC resonant converters and bidirectional power flow in current power electronics systems. The

study may address the bidirectional isolated LLC resonant converter's design, components, and operation. The report may discuss experimental validation or modeling of the converter's efficiency, power density, and performance. This study shows how to develop efficient LLC resonant bidirectional power converters, advancing power electronics.

Y. Qiu, W. Liu, P. Fang, Y. F. Liu, and P. C. Sen released a mathematical guide for building an AC-DC LLC converter with Power Factor Correction in 2018. PFC may be highlighted in power converters for efficiency and regulatory compliance in the abstract. The study may design the LLC converter with PFC by selecting components, controlling, and optimizing performance. The investigation may include examine converter operating and performance mathematical models and design equations. The study helps engineers and researchers construct efficient and high-performance LLC-PFC AC-DC power converters.

4. RELATED WORK

DESIGN CONSTRAINTS

The design of the converter has the following limitations:

- Input voltage: (300-320 V_{DC});
- Rated power: 225 W;
- Output voltage range (3-5 V);
- Maximum output current: 45 A (in correspondence of 5V of voltage output);
- Output Voltage line regulation $\leq 1\%$ ($V_{in}=320$ V);
- Output voltage ripple ≤ 120 mV;
- Switching frequency (100-150kHz).

It is thought that the electricity coming from the single-phase grid is from a full-wave rectifier, and it is roughly 300–320 VDC. The maximum power is produced at 45 A of current when the voltage is 5 V. For the electrolyzer to work correctly, the

switching frequency needs to be higher than 100 kHz in order to guarantee that the voltage disturbance is kept to a minimum. This also makes it possible to use an efficient high-frequency transformer. It is important to note that the load is only represented as resistive; the dynamic behavior would also need to be included in the comprehensive model shown in [27]. However, since the dynamic behavior affects just transients, the simpler method works well for the steady-state study.

Choice of the components

The plan was executed according to the procedures outlined. The subsequent criteria are implemented for the purpose of selection: It guarantees a linear control interval of sufficient quality with $L_n=5$ and $Q_e=0.35$.

The gain curve depicted in Figure 5 was generated using this collection of numbers. It is evident that the gain decreases in a linear manner as the frequency increases within the operating frequency range of 110–150 kHz. The resonance frequency has been determined to be 130 kHz. The change frequency is also employed to simplify the filtering design, thereby reducing electromagnetic interference (EMI).

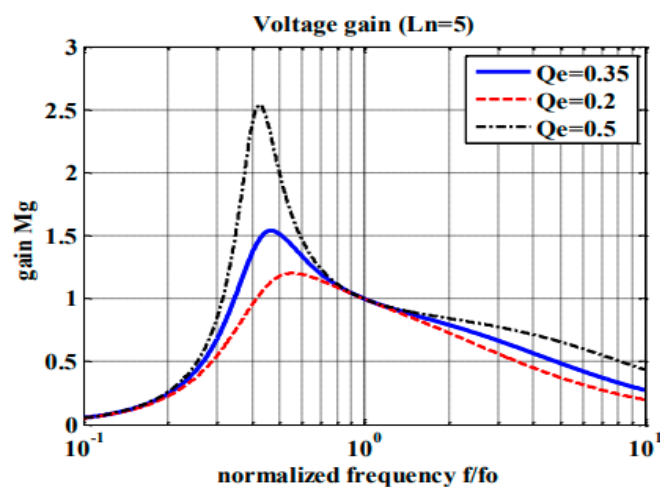


Fig. 5. Normalized converter gain vs. frequency

Table 1 provides an exhaustive list of the components that have been incorporated. It is important to note that the output capacitor was

acquired via a parallel connection in order to reduce ESR and associated losses. To achieve the desired reduction ratio, an adequate core is coiled around the high frequency transformer.

Symbol	Rated value	Supplier	Code
MOSFET (x2)	650V, 5.5A	Infineon	IPP65R420CFD
Diode (x2)	0.79V, 70A	IXYS	DSA70C200HB
Lr	39 μH	Bourns	2100LL-390-RC
Cr	38 nF	Würth	WCAP-FTXX Film Capacitor
Co (x9)	100 μF	KEMET	C1006-X5R-SMD
Transformer	19:1:1	TDK-Epcos	PQ35/35 core
VCO		LT	LTC6990
Driver		LT	LT1162

4. RESULTS AND ANALYSIS

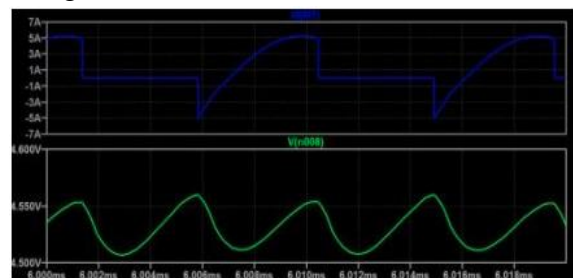
The converter's efficacy at 110, 130, and 150 kHz is demonstrated by the LTspice simulator results. The incoming current (top view) and output voltage (bottom view) are illustrated in Figure 6. It is feasible, in fact. The output voltage is within a 1% range of 4.5 V to 2.64 V. The current situation is illustrated in Figure 7.

The rectifier diodes, I(D2) and I(D3), are visible in the top and bottom perspectives. The magnetizing current I_m increases the resonant current I_r . As anticipated, the switching frequency decreases as all currents diminish. The gentle switching of diodes at zero current, which occurs above the resonance frequency, is illustrated in Figure 8.

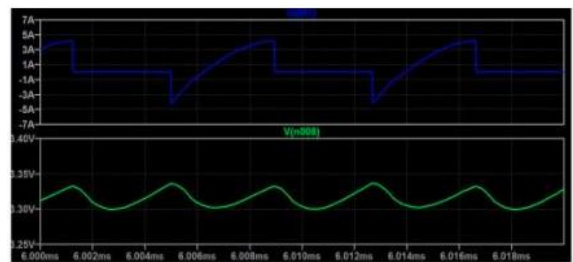
The voltage across the drain and source of the MOSFET Q2 is depicted in the top image of Figure 9, while the voltage across the MOSFET gate is depicted in the bottom picture. ZVS is able to commute as a result of the idle time.

The converter's dynamic behavior was illustrated by a gradual modification in the switching

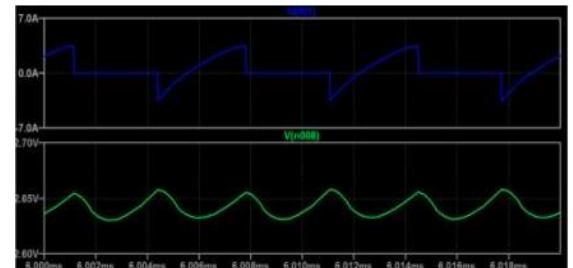
frequency. In Figures 10 and 11, the output voltage fluctuates as the control frequency transitions from 140 kHz to 120 kHz and back again. The converter is designed to maintain the electrolyzer's functionality by providing an appropriate level of overdamping to prevent vibrations from generating an inordinate amount of voltage.



fs=110 kHz

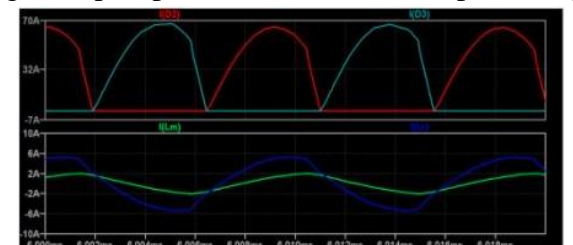


fs=130 kHz

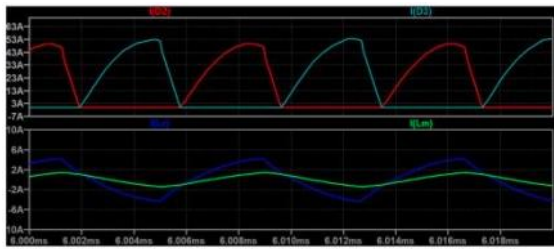


fs=150 kHz

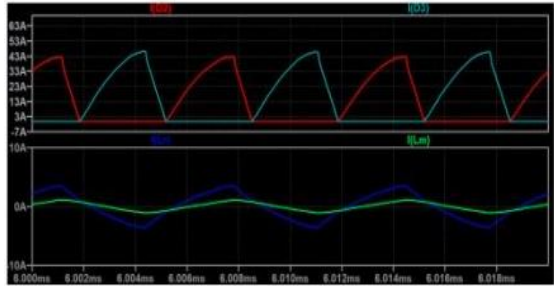
Fig. 6. top: input current, bottom: output voltage



fs=110 kHz

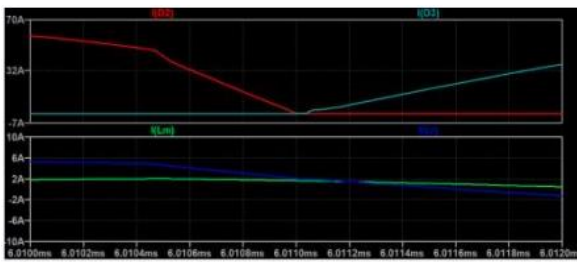


fs=130 kHz

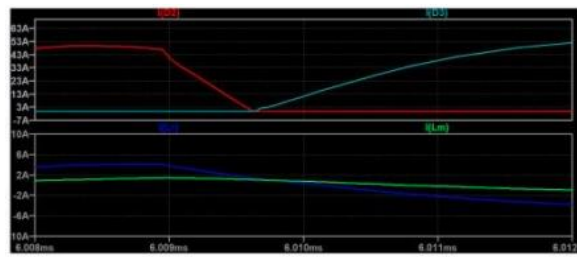


fs=150 kHz

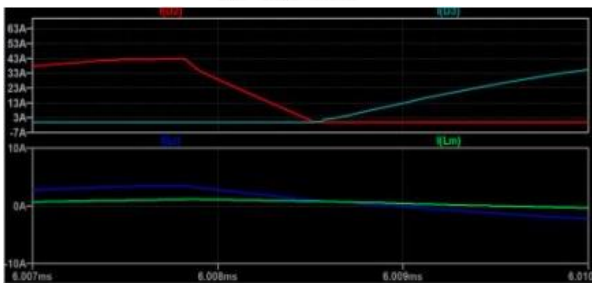
Fig. 7. Top rectifier diode current and bottom magnetizing current resonant.



fs=110 kHz

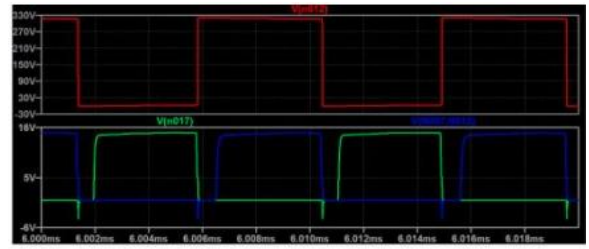


fs=130 kHz

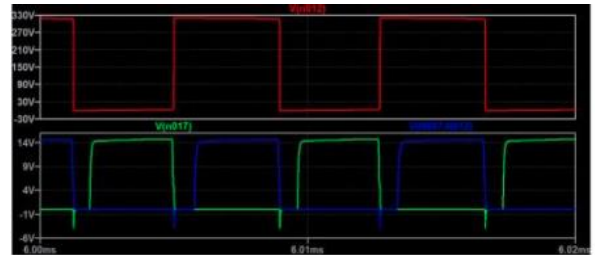


fs=150 kHz

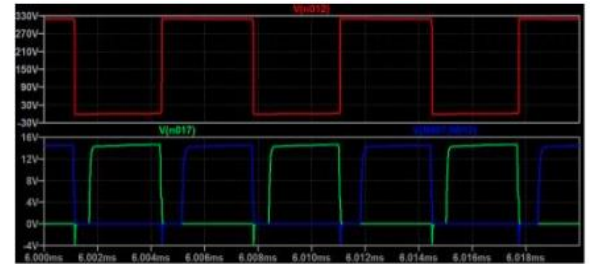
Figure 8. Zoom of figure 7 to illustrate diode soft commutation.



fs=110 kHz



fs=130 kHz



fs=150 kHz

Fig. 9. Top: MOSFET Q2 drain-to-source voltage; bottom: gate voltage

A PI regulator can maintain an overdamped response through feedback when a dominant pole approaches the dynamic response. Conduction losses in the diode, switching and conduction losses on the two MOSFETs, joule losses on the inductor L_r , capacitor C_r , and co-capacitor C_o , as well as the minor but significant joule and magnetic losses in the transformers, were all taken into consideration in order to determine the converter's efficiency. In Figure 12, losses relative to total power are displayed. In Figure 13, total efficiency and output power are related. There are significant financial losses in the conductors of diodes with high current levels. A synchronous rectifier can reduce losses and boost efficiency by up to 75% when operating at maximum power.

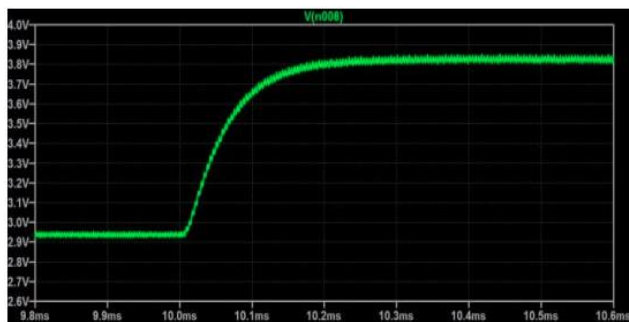


Fig. 10. Output voltage with 140–120 kHz input frequency steps.

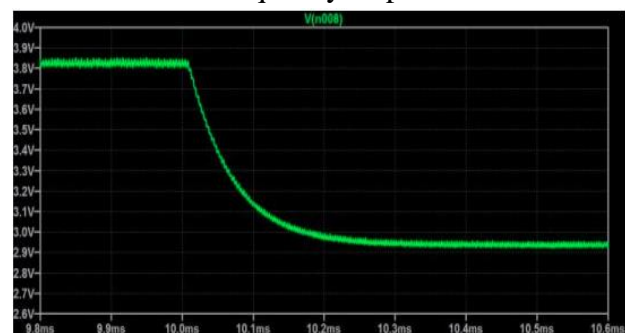


Fig. 11. Output voltage with 120–140 kHz input frequency steps.

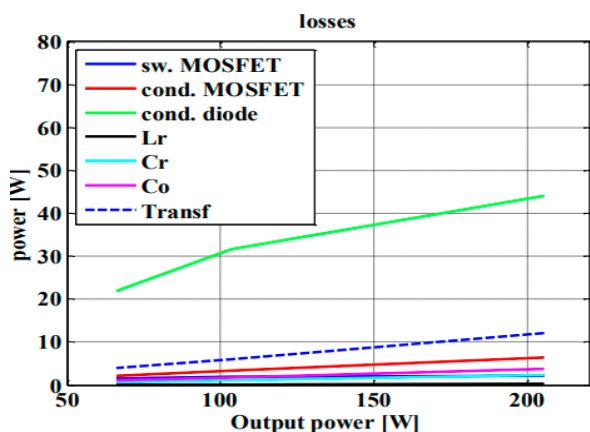


Fig. 12. Losses vs. frequency of the converter's components

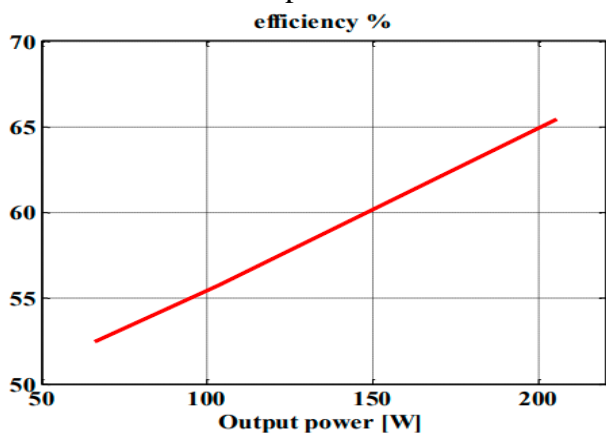


Fig. 13. Efficiency vs. output power of the converter.

5. CONCLUSION

A PEM electrolyzer can be used with an LLC resonance converter. By letting a high voltage drop ratio happen, the converter lowers the overall stress on the MOSFETs. It also makes sure that the operational voltage stays within the electrolyzer's working range, that the output voltage doesn't change too much, and that the dynamic reaction isn't too dampened.

By lowering switching and backward recovery losses, this architecture makes things less efficient. The main reason for this drop is the high output current, which causes the converter to lose some of its power.

REFERENCES

1. Yodwong, B., Guilbert, D., Phattanasak, M., Kaewmanee, W., Hinaje, M., & Vitale, G. (2020). Proton Exchange Membrane Electrolyzer Modeling for Power Electronics Control: A Short Review. C—Journal of Carbon Research, 6(2), 29.
2. Hiva Kumar, S.; Himabindu, V. Hydrogen production by PEM water electrolysis—A review. Mater. Sci. Energy Technol. 2019, 2, 442–454.
3. Nikolaidis, P.; Poullikkas, A. A comparative overview of hydrogen production processes. Renew. Sustain. Energy Rev. 2017, 67, 597–611.
4. Carmo, M.; Fritz, D.; Mergel, J.; Stolten, D. A comprehensive review on PEM water electrolysis. Int. J. Hydrogen Energy 2013, 38, 4901–4934.
5. Falcão, D.; Pinto, A. A review on PEM electrolyzer modelling: Guidelines for beginners. J. Clean. Prod. 2020, 261, 121184.
6. Yodwong, B., Guilbert, D., Phattanasak, M., Kaewmanee, W., Hinaje, M., & Vitale, G.

- (2020). AC-DC converters for electrolyzer applications: State of the art and future challenges. *Electronics*, 9(6), 912.
7. Solanki, J.; Wallmeier, P.; Böcker, J.; Averberg, A.; Fröhleke, N. High-current variable-voltage rectifiers: State of the art topologies. *IET Power Electron.* 2015, 8, 1068–1080.
 8. Solanki, J.; Fröhleke, N.; Böcker, J.; Wallmeier, P. Comparison of Thyristor-Rectifier with Hybrid Filter and Chopper-Rectifier for High-Power, High-Current Application.
 9. In Proceedings of the PCIM Europe, Nuremberg, Germany, 14–16 May 2013; pp. 1391–1398.
 10. Rodriguez, J.; Pontt, J.; Silva, C.; Wiechmann, E.; Hammond, P.; Santucci, F.; Alvarez, R.; Musalem, R.; Kouro, S.; Lezana, P. Large Current Rectifiers: State of the Art and Future Trends. *IEEE Trans. Ind. Electron.* 2005, 52, 738–746.
 11. Solanki, J.; Frohleke, N.; Bocker, J. Implementation of Hybrid Filter for 12-Pulse Thyristor Rectifier Supplying High-Current Variable-Voltage DC Load. *IEEE Trans. Ind. Electron.* 2015, 62, 4691–4701.
 12. Koponen, J.; Ruuskanen, V.; Kosonen, A.; Niemela, M.; Ahola, J. Effect of Converter Topology on the Specific Energy Consumption of Alkaline Water Electrolyzers. *IEEE Trans. Power Electron.* 2019, 34, 6171–6182.
 13. Dobó, Z.; Palotás, Á. Impact of the current fluctuation on the efficiency of Alkaline Water Electrolysis. *Int. J. Hydrogen Energy* 2017, 42, 5649–5656.
 14. Ruuskanen, V.; Koponen, J.; Kosonen, A.; Niemelä, M.; Ahola, J.; Hämäläinen, A. Power quality and reactive power of water electrolyzers supplied with thyristor converters. *J. Power Sources* 2020, 459, 228075.
 15. Topic Category: Design Reviews – Functional Circuit locks,—Designing an LLC Resonant Half-Bridge Power Converter, available on: <https://www.ti.com/seclit/ml/slup263/slup263.pdf> (accessed on March the 9th, 2021).
 16. Jung, J. H., & Kwon, J. G. (2007, September). Theoretical analysis and optimal design of LLC resonant converter. In 2007 European Conference on Power Electronics and Applications (pp. 1-10). IEEE.
 17. Hillers, A., Christen, D., & Biela, J. (2012, September). Design of a highly efficient bidirectional isolated LLC resonant converter. In 2012 15th International Power Electronics and Motion Control Conference (EPE/PEMC) (pp. DS2b-13). IEEE.
 18. Qiu, Y., Liu, W., Fang, P., Liu, Y. F., & Sen, P. C. (2018, March). A mathematical guideline for designing an AC-DC LLC converter with PFC. In 2018 IEEE Applied Power Electronics Conference and Exposition (APEC) (pp. 2001-2008). IEEE.